The Journal of Chemical Physics

Comparing correlation components and approximations in Hartree–Fock and Kohn–Sham theories via an analytical test case study

Cite as: J. Chem. Phys. **157**, 054102 (2022); https://doi.org/10.1063/5.0097095
Submitted: 25 April 2022 • Accepted: 27 June 2022 • Published Online: 03 August 2022

Sara Giarrusso and Aurora Pribram-Jones

The Journal of Chemical Physics ARTICLE scitation.org/journal/jcp

Comparing correlation components and approximations in Hartree–Fock and Kohn–Sham theories via an analytical test case study

Cite as: J. Chem. Phys. 157, 054102 (2022); doi: 10.1063/5.0097095
Submitted: 25 April 2022 • Accepted: 27 June 2022 •
Published Online: 3 August 2022

Sara Giarrusso and Aurora Pribram-Jones[a)]

AFFILIATIONS

Department of Chemistry and Biochemistry, University of California Merced, 5200 North Lake Rd., Merced, California 95343, USA

Note: This paper is part of the 2022 JCP Emerging Investigators Special Collection.
[a)]**Author to whom correspondence should be addressed:** apj@ucmerced.edu

ABSTRACT

The asymmetric Hubbard dimer is a model that allows for explicit expressions of the Hartree–Fock (HF) and Kohn–Sham (KS) states as analytical functions of the external potential, Δv, and of the interaction strength, U. We use this unique circumstance to establish a rigorous comparison between the individual contributions to the correlation energies stemming from the two theories in the $\{U, \Delta v\}$ parameter space. Within this analysis of the Hubbard dimer, we observe a change in the sign of the HF kinetic correlation energy, compare the indirect repulsion energies, and derive an expression for the "traditional" correlation energy, i.e., the one that corrects the HF estimate, in a pure site-occupation function theory spirit [Eq. (45)]. Next, we test the performances of the Liu–Burke and the Seidl–Perdew–Levy functionals, which model the correlation energy based on its weak- and strong-interaction limit expansions and can be used for both the traditional and the KS correlation energies. Our results show that, in the Hubbard dimer setting, they typically work better for the HF reference, despite having been originally devised for KS. These conclusions are somewhat in line with prior assessments of these functionals on various chemical datasets. However, the Hubbard dimer model allows us to show the extent of the error that may occur in using the strong-interaction ingredient for the KS reference in place of the one for the HF reference, as has been carried out in most of the prior assessments.

I. INTRODUCTION AND THEORETICAL BACKGROUND

Electronic structure problems in chemistry can be addressed via an ever-increasing variety of methods, inviting both explicit and implied comparisons. The various methods are sometimes classified into the wavefunction-based category or the density functional theory (DFT) one. A large part of this work is devoted to comparing the "primal" wavefunction method, i.e., Hartree–Fock (HF), and the most popular flavor of DFT, i.e., Kohn–Sham (KS).

These methods have been known for a very long time and, in recent years, the number of works that combine them has been increasing.[1–4] However, a systematic comparison of the two, contrasting their formal properties and guiding new approaches that combine them, is quite a hard task. A fair comparison, such as the one done in Ref. 5 for three simple diatomic molecules, requires the calculation of extremely accurate *ab initio* wavefunctions from which the exact KS quantities [wavefunction, exchange-correlation (XC) energy, etc.] may be constructed. In addition, this procedure is system-specific: it has to be repeated for any system for which one wishes to investigate how the two methods compare to one another, complicating systematic studies. Furthermore, the effect of the basis set used can hardly be identical in the HF and the KS states, introducing errors in the comparison. We bypass these disadvantages by adopting a radically simple model system: the asymmetric Hubbard dimer. In this model, both the HF and the KS states can be constructed analytically. A comparison of the *exact* correlation energies stemming from the two theories within this model is carried out in Sec. II.

A parallel focus of this work lies in testing certain *approximations* for the correlation energy. Despite the definition of the correlation energy depending on the chosen method, our investigation focuses on the performances of the Liu–Burke[6] (LB) and Seidl–Perdew–Levy[7] (SPL) functionals that approximate this energy,

interpolating between its weak- and strong-interaction limit expansions. As such, these functionals can be adopted for different types of correlation energies with the same rationale. The results of this investigation are reported in Sec. III.

In the remainder of this section, we review the Hubbard dimer model (Sec. I A), the HF and the KS theories (Sec. I B), and the interpolations used (Sec. I C). Before going through each of these, let us introduce the usual non-relativistic Hamiltonian expression considered in electronic structure calculations,

$$\hat{H} = \hat{T} + \hat{V}_{ee} + \hat{V}, \tag{1}$$

where $\hat{T} = -\sum_i^N \frac{\nabla_i^2}{2}$ is the kinetic energy operator, N is the number of particles in the system, $\hat{V}_{ee}$ represents the Coulomb interaction between all electron pairs, and $\hat{V} = \sum_i^N v(i)$ is the N-particle sum of the external potential, (typically) given by the positive field of the nuclei, felt by each electron. Let $|\Psi\rangle$ be the wavefunction that solves the Schrödinger equation defined by $\hat{H}$ with the lowest eigenvalue E. The solution, $|\Psi\rangle$, is notoriously hard to find, as it depends on the spatial and spin variables of each particle, i.e., $|\Psi\rangle = \Psi(\mathbf{x}_1, \ldots, \mathbf{x}_N)$, with $\mathbf{x}_i = \mathbf{r}_i\sigma_i$ being the spatial and spin coordinates. On the other hand, the ground-state (GS) electron probability density, or just (electron) density, is

$$n(\mathbf{r}) := \langle\Psi|\hat{n}|\Psi\rangle, \tag{2}$$

where $\hat{n} = \sum_i^N \delta(\mathbf{r}_i - \mathbf{r})$ and the Dirac brackets $\langle\cdots|\cdots\rangle$ stand for $\int d\mathbf{x}_1 \cdots d\mathbf{x}_N$, with $\int d\mathbf{x} = \sum_\sigma \int d\mathbf{r}$ being a much simpler mathematical object.

Furthermore, if the ground state is unique, there is a bijective mapping between the wavefunction Ψ and the external potential v, and by virtue of Eq. (2), also between n and v, so that the expectation value of a suitable operator $\hat{A}$ evaluated on the GS wavefunction is also a functional of the GS density,

$$A[n] = \langle\Psi[n]|\hat{A}|\Psi[n]\rangle. \tag{3}$$

A. The asymmetric Hubbard dimer

The general N-site Hubbard model was originally studied to describe the correlation effects in partially filled narrow energy bands in solids.[8–10] It has gradually been used in the most diverse sceneries of physics and chemistry and is now often used as a playground to test new computational methods or concepts.[11–13] Its two-site asymmetric version is relevant in the context of density functional theory,[14–16] or Site Occupation Function Theory (SOFT) as is called in the lattice setting, and its offshoots (time-dependent DFT,[17] density embedding theory,[18] ensemble DFT,[19] and thermal DFT[20]). Its simplicity allows a detailed, controlled, and not rarely analytical exploration of the quantities of interest in these fields.

The two-site Hubbard model Hamiltonian reads as follows:

$$\hat{\mathscr{H}} = \hat{\mathscr{T}} + \hat{\mathscr{U}} + \hat{\mathscr{V}}, \tag{4}$$

where

$$\hat{\mathscr{T}} = -t\sum_\sigma \left(\hat{a}_{0\sigma}^\dagger \hat{a}_{1\sigma} + \hat{a}_{1\sigma}^\dagger \hat{a}_{0\sigma}\right), \tag{5}$$

$$\hat{\mathscr{U}} = U\sum_{i=0,1} \hat{n}_{i\uparrow}\hat{n}_{i\downarrow}, \tag{6}$$

$$\hat{\mathscr{V}} = \sum_{i=0,1} v_i \hat{n}_i, \tag{7}$$

where $\hat{a}^\dagger$, $\hat{a}$ are the usual creation and annihilation operators, $\sigma = \uparrow, \downarrow$ labels the spin of the particles, $i = 0, 1$ labels the two sites, and $\hat{n}_{i\sigma} = \hat{a}_{i\sigma}^\dagger \hat{a}_{i\sigma}$ and $\hat{n}_i = \hat{n}_{i\sigma} + \hat{n}_{i\bar{\sigma}}$ (with $\bar{\sigma}$ being the spin opposite to σ) are the occupation operators. The parameters appearing in the Hamiltonian, namely, t, U, and $\{v_i\}$, determine the aptitude of the particles to hop on the other site, the strength of the repulsion between particles, and their attraction to each site, respectively. In this sense, each term in the lattice Hamiltonian mimics the action of each term in the electronic Hamiltonian [Eq. (1)].

The eigenstates corresponding to Eq. (4) are fully determined by the reduced variables $u = \frac{U}{2t}$ and $\delta v = \frac{\Delta v}{2t}$, with $\Delta v = v_1 - v_0$. Thus, we set $t = 1/2$ throughout the paper, as is customary.[14] Furthermore, we constrain the expectation value of the occupation operators on each site, n_i, to add up to two (i.e., $n_0 + n_1 = 2$), and we consider only the states with $S_z = 0$. Therefore, the Fock space reduces to three-dimensions and can be represented by the basis $|0\uparrow\,0\downarrow\rangle, |1\uparrow\,1\downarrow\rangle$ and the antisymmetric combination of singly occupied sites $\frac{1}{\sqrt{2}}(|0\uparrow 1\downarrow\rangle - |0\downarrow 1\uparrow\rangle)$. The associated Schrödinger equation can be solved analytically by finding the roots of a cubic polynomial, and all the quantities of interest can be compactly expressed by trigonometric formulas. Note that, although we can generally express how the occupation difference $\Delta n = n_1 - n_0$ depends on U and Δv, the inverse mapping (i.e., $\Delta n \to \Delta v$) is not analytical.

We stress two fundamental features of $\hat{\mathscr{H}}$, which set it apart from the electronic Hamiltonian of Eq. (1): the first one is that the lack of a (second-order) derivative with respect to the particle space variable significantly alters the meaning of "kinetic energy" in the quantum context (no Heisenberg principle, wave-particle duality, and so on). In fact, the expectation value of the hopping operator is negative. The second is that the two-body interaction in the lattice model is defined only between particles with opposite spin, a relevant difference from electrons, which interact with one another regardless of their spin. Therefore, the mean-field term [Eq. (14) below] in the Hubbard model is free of the self-interaction error. Similarly, the exchange energy [Eq. (15) below], which specifically accounts for the interaction among particles of the same spin, is exactly zero. Correspondingly, in this work, we choose to compare the two theories, HF and KS, only in their correlation energy contributions. See also Sec. II A for a more detailed discussion of these choices. To set the stage for the comparison between the two theories, we review them in general terms in Sec. I B.

B. Hartree–Fock and Kohn–Sham methods

According to the Hartree–Fock method, the expectation value of the Hamiltonian in Eq. (1) is minimized in the space of Slater determinants, $\Phi := \sum_P (-1)^P \psi_{P(1)}(\mathbf{x}_1)\cdots\psi_{P(N)}(\mathbf{x}_N)$, where the $\psi_n(\mathbf{x})$ are single-particle wavefunctions and the spatial and spin coordinates are considered separable, i.e., $\psi_n(\mathbf{x}) \equiv \phi_n(\mathbf{r})s_n(\sigma)$, while the index P lists all possible permutations. Its ground state is then given by

$$|\Phi^{\mathrm{HF}}\rangle = \mathrm{argmin}_\Phi \langle\Phi|\hat{H}|\Phi\rangle. \tag{8}$$

The corresponding ground-state density, $n^{\mathrm{HF}}(\mathbf{r}) = \sum_\sigma \sum_i^N |\psi_i^{\mathrm{HF}}(\mathbf{x})|^2$, typically differs from the interacting one [Eq. (2)]. The HF approximation to the GS energy is

$$E^{\mathrm{HF}} := \langle \Phi^{\mathrm{HF}} | \hat{H} | \Phi^{\mathrm{HF}} \rangle, \tag{9}$$

and, by virtue of the variational principle, $E^{\mathrm{HF}} \geq E$. Their difference is usually referred to as simply the "correlation energy," E_c; however, we shall label it the Hartree–Fock correlation energy, E_c^{HF}, to distinguish it from the KS one. It is defined as the difference between the GS energy and its HF approximation, E^{HF}, and consists of the following individual contributions:

$$E_c^{\mathrm{HF}} = T_c^{\mathrm{HF}} + U_c^{\mathrm{HF}} + V_c^{\mathrm{HF}}, \tag{10}$$

where

$$T_c^{\mathrm{HF}} := T[n] - T^{\mathrm{SD}}[\{\psi_i^{\mathrm{HF}}\}], \tag{11}$$

$$U_c^{\mathrm{HF}} := V_{ee}[n] - U_H[n^{\mathrm{HF}}] - E_x[\{\psi_i^{\mathrm{HF}}\}], \tag{12}$$

$$V_c^{\mathrm{HF}} := V[n] - V[n^{\mathrm{HF}}]. \tag{13}$$

Here, the first terms on the right-hand side of Eqs. (11)–(13) are applications of Eq. (3), while $T^{\mathrm{SD}}[\{\psi_i\}] = \frac{1}{2}\sum_i^N \int |\nabla_{\mathbf{r}} \psi_i(\mathbf{x})|^2 \mathrm{d}\mathbf{x}$ is the kinetic energy as evaluated on a Slater determinant,

$$U_H[n] := \frac{1}{2} \iint \frac{n(\mathbf{r}) n(\mathbf{r}')}{|\mathbf{r} - \mathbf{r}'|} \mathrm{d}\mathbf{r}\mathrm{d}\mathbf{r}' \tag{14}$$

is the mean field repulsion energy, and

$$E_x[\{\psi_i\}] = -\frac{1}{2} \sum_{ij}^N \iint \frac{\psi_i^*(\mathbf{x}) \psi_j^*(\mathbf{x}') \psi_i(\mathbf{x}') \psi_j(\mathbf{x}')}{|\mathbf{r} - \mathbf{r}'|} \mathrm{d}\mathbf{x}\mathrm{d}\mathbf{x}' \tag{15}$$

is the exchange energy that is derived by evaluating the interaction operator on a Slater determinant and subtracting the mean-field term. Moreover, the external potential energy functional is a simple explicit functional of the density, $V[n] := \int v(\mathbf{r}) n(\mathbf{r}) \mathrm{d}\mathbf{r}$.

In the Kohn–Sham formulation of DFT, the full Hamiltonian is set aside and only the kinetic energy operator is minimized over all antisymmetric N-particle wavefunctions. However, the minimization is performed under the constraint of a fixed density. The resulting density functional is known as the Kohn–Sham kinetic energy functional,

$$T_s[n] := \min_{\Psi \to n} \langle \Psi | \hat{T} | \Psi \rangle. \tag{16}$$

The minimizing wavefunction is expected to be a Slater Determinant, as there are no two-body operators entering the minimization, although there are cases in which the single Slater determinant description cannot deliver the prescribed density.[21–23] If we neglect such cases, then $T_s[n] \equiv T^{\mathrm{SD}}[\{\psi_i^{\mathrm{KS}}\}]$, where the KS orbitals $\{\psi_i^{\mathrm{KS}}\}$ are the one-particle functions cast in the KS Slater determinant, Φ^{KS}, which is the minimizer of the search on the right-hand side of Eq. (16). The KS orbitals are clearly functionals of the density but in an implicit and highly non-trivial way. Conversely, the interacting density is easily written in terms of the KS orbitals as $n(\mathbf{r}) = \sum_\sigma \sum_i^N |\psi_i^{\mathrm{KS}}(\mathbf{x})|^2$. The correlation energy according to KS-DFT, E_c^{KS}, is given by

$$E_c^{\mathrm{KS}} = T_c^{\mathrm{KS}} + U_c^{\mathrm{KS}}, \tag{17}$$

where T_c^{KS} and U_c^{KS} look formally identical to Eqs. (11) and (12), respectively, with the "non-interacting" pieces having the KS orbitals $\{\psi_i^{\mathrm{KS}}\}$ and the interacting density as input rather than the HF quantities. The missing external potential contribution in Eq. (17) compared to Eq. (10) is a result of the KS density being, by construction, equal to the interacting one. This is at the root of KS-DFT being an exact treatment rather than an approximation strategy like Hartree–Fock. The matching between the density of the "non-interacting" auxiliary system and that of the interacting target system is enforced by means of an effective external potential, called the KS potential, v_s. To see the relation between said potential and Eq. (17), one may decompose it into

$$v_s = v + v_H + v_{xc}, \tag{18}$$

where v is the external potential of the target problem [Eq. (1)], v_H is the Hartree potential defined as the functional derivative of $U_H[n]$, i.e., $v_H[n](\mathbf{r}) = \int \frac{n(\mathbf{r}')}{|\mathbf{r}-\mathbf{r}'|} \mathrm{d}\mathbf{r}'$, and v_{xc} is the so-called exchange-correlation (XC) potential and corresponds to the functional derivative of the XC energy

$$v_{xc}[n_0] = \left. \frac{\delta E_{xc}^{\mathrm{KS}}[n]}{\delta n} \right|_{n=n_0}, \tag{19}$$

with $E_{xc}^{\mathrm{KS}}[n] = E_c^{\mathrm{KS}}[n] + E_x[\{\psi_i^{\mathrm{KS}}\}[n]]$.

In general, as E_{xc}^{KS} is not known, this term has to be approximated in actual KS-DFT calculations. Although we have access to the numerically exact quantity for our Hubbard dimer, we present one possible route to build approximations for it in Sec. I C.

C. Approximations from the adiabatic connection framework

A quite powerful and long-established tool to construct approximation for the XC energy in KS-DFT is represented by the density-fixed adiabatic connection formalism.[24–27] According to this formalism, a parameter λ is used to tune the strength of the interaction operator in the Hamiltonian (1) while keeping the density fixed, under the assumption that the density is v-representable for all λ, i.e.,

$$\hat{H}_\lambda^{\mathrm{KS}} = \hat{T} + \lambda \hat{V}_{ee} + \hat{V}^\lambda, \tag{20}$$

where $\hat{V}^\lambda = \sum_i^N v^\lambda(\mathbf{r}_i)$ and v^λ is the Lagrange multiplier that keeps the density fixed at each λ. One can then show that

$$E_{xc}^{\mathrm{KS}}[n] = \int_0^1 W_\lambda^{\mathrm{KS}}[n] \mathrm{d}\lambda, \tag{21}$$

with the AC integrand defined as

$$W_\lambda^{\mathrm{KS}}[n] := \langle \Psi_\lambda^{\mathrm{KS}}[n] | \hat{V}_{ee} | \Psi_\lambda^{\mathrm{KS}}[n] \rangle - U_H[n], \tag{22}$$

and with $\Psi_\lambda^{\mathrm{KS}}$ being the ground state of the λ-dependent Hamiltonian (20) at each λ.

The exact behavior of W_λ^{KS} is known locally in the two limits $\lambda \to 0$[28,29] and $\lambda \to \infty$,[30,31]

$$W_{\lambda \to 0}^{\mathrm{KS}}[n] = E_x[\{\psi_i^{\mathrm{KS}}[n]\}] + \sum_{\mathrm{n}=2}^{\infty} \mathrm{n}\, E_c^{\mathrm{GLn}} \lambda^{\mathrm{n}-1}, \tag{23}$$

$$W^{\mathrm{KS}}_{\lambda\to\infty}[n] = W^{\mathrm{KS}}_{\infty}[n] + O\left(\lambda^{-\frac{1}{2}}\right), \tag{24}$$

where E_c^{GLn} are the nth-order Görling–Levy (GL) correlation energy coefficients[28,29] and W^{KS}_{∞} is the minimal repulsion energy in a given density removed of its mean-field part.[30,32]

Models for the KS-DFT XC energy based on interpolation between the weak- and the strong-interaction expansions, Eqs. (23) and (24), respectively, are called Adiabatic Connection Interaction Interpolations (ACIIs) or Adiabatic Connection Methods (ACMs). In fact, these approximations, developed within KS-DFT, have been successfully used with HF ingredients as a correction to the HF energy.[33–36] Such practice began from the simple heuristic observation that using ACMs on HF ingredients gave consistently better results than using them on KS ones.[33]

While adaptations of the adiabatic connection approach to wavefunction methods had already begun to appear (see Ref. 37 and references therein), the key factor needed to justify the use of ACMs with different reference states was the boundedness of the leading coefficient in the strong-interaction expansion of the corresponding AC integrand. In the case of the AC with the HF state as reference, such boundedness was shown only more recently.[38]

Within this other adiabatic connection framework, the λ-dependent Hamiltonian reads

$$\hat{H}^{\mathrm{HF}}_{\lambda} = \hat{T} + \hat{V}_{\mathrm{HF}} + \hat{V} + \lambda\left(\hat{V}_{ee} - \hat{V}_{\mathrm{HF}}\right), \tag{25}$$

where $\hat{V}_{\mathrm{HF}} = \sum_{i,j}^{N}\left(\hat{J}^{\mathrm{HF}}_j(\mathbf{x}_i) - \hat{K}^{\mathrm{HF}}_j(\mathbf{x}_i)\right)$,

$$\hat{J}^{\mathrm{HF}}_i(\mathbf{x}) = \int \frac{|\psi^{\mathrm{HF}}_i(\mathbf{x})|^2}{|\mathbf{r}-\mathbf{r}'|}\,\mathrm{d}\mathbf{x}', \tag{26}$$

and

$$\hat{K}^{\mathrm{HF}}_i(\mathbf{x})\phi(\mathbf{x}) = \psi^{\mathrm{HF}}_i(\mathbf{x}) \int \frac{\psi^{\mathrm{HF}*}_i(\mathbf{x}')\,\phi(\mathbf{x}')}{|\mathbf{r}-\mathbf{r}'|}\,\mathrm{d}\mathbf{x}'. \tag{27}$$

Similar to the DFT case, one can show that

$$E^{\mathrm{HF}}_c = \int_0^1 W^{\mathrm{HF}}_{\lambda}\mathrm{d}\lambda, \tag{28}$$

with the adiabatic connection integrand, $W^{\mathrm{HF}}_{\lambda}$, defined as

$$W^{\mathrm{HF}}_{\lambda} := \langle\Psi^{\mathrm{HF}}_{\lambda}|\hat{V}_{ee} - \hat{V}_{\mathrm{HF}}|\Psi^{\mathrm{HF}}_{\lambda}\rangle + c^{\mathrm{HF}}_0[n^{\mathrm{HF}}], \tag{29}$$

and $c^{\mathrm{HF}}_0[n^{\mathrm{HF}}] = U_H[n^{\mathrm{HF}}] + E_x[\{\psi^{\mathrm{HF}}_i\}]$. Note that we have decided to shift $W^{\mathrm{HF}}_{\lambda}$ such that it integrates to the correlation energy alone. As a result of this choice, the exchange term does not appear in Eq. (30), in contrast with the analogous small-λ expansion [Eq. (23)] of the DFT AC integrand.

The small- and large-λ expansions of $W^{\mathrm{HF}}_{\lambda}$ give

$$W^{\mathrm{HF}}_{\lambda\to 0} = \sum_{\mathrm{n}=2}^{\infty} \mathrm{n}\, E_c^{\mathrm{MPn}}\lambda^{\mathrm{n}-1}, \tag{30}$$

$$W^{\mathrm{HF}}_{\lambda\to\infty} = W^{\mathrm{HF}}_{\infty} + O\left(\lambda^{-\frac{1}{2}}\right), \tag{31}$$

where E_c^{MPn} are the nth-order Møller–Plesset (MP) correlation coefficients and

$$W^{\mathrm{HF}}_{\infty} = E_{el}[n^{\mathrm{HF}}] + E_x[\{\psi^{\mathrm{HF}}_i\}], \tag{32}$$

with

$$E_{\mathrm{el}}[n] \equiv \min_{\{\mathbf{r}_1,\ldots,\mathbf{r}_N\}}\left\{\sum_{i,j>i}^{N}\frac{1}{|\mathbf{r}_i-\mathbf{r}_j|} - \sum_{i=1}^{N} v_{\mathrm{H}}(\mathbf{r}_i;[n]) + U_H[n]\right\} \tag{33}$$

being the minimum total electrostatic energy of N equal classical point charges $(-e)$ in a positive background with continuous charge density $(+e)n(\mathbf{r})$.[38]

The ACMs strategy of interpolating between the weak- and the strong-interaction expansions of the desired AC integrand has the major merit of providing an all-order resummation of the perturbation series coefficients by encompassing also the strong-interaction information. This avoids difficulties such as slowly convergent or divergent series (see, e.g., a discussion of the shortcomings associated with MP theory in quantum chemistry in Ref. 39).

In this work, we test two ACMs that depend on three ingredients: E_x; E_c^{PT2}, where "PT" stands for "Perturbation Theory"; and W_∞. Note that, while the ingredient E_x is formally exactly the same regardless of the reference used (HF or KS) and only the input quantities change (i.e., HF or KS orbitals), the ingredients E_c^{PT2} and W_∞ correspond, respectively, to E_c^{MP2} and W^{HF}_{∞} for the HF reference, and E_c^{GL2} and W^{KS}_{∞} for the KS reference.

Specifically, the functionals considered in this work are the Liu–Burke (LB),[6]

$$E_c^{\mathrm{LB}} = -\frac{\tilde{W}^2_{\infty}\left(\sqrt{\frac{20W'_0}{\tilde{W}_{\infty}}+25}-5\right)}{4W'_0} - \frac{5\tilde{W}^2_{\infty}}{8W'_0+10\tilde{W}_{\infty}} + \tilde{W}_{\infty}, \tag{34}$$

and the Seidl–Perdew–Levy (SPL),[7]

$$E_c^{\mathrm{SPL}} = \tilde{W}_{\infty} - \frac{\tilde{W}^2_{\infty}\left(\sqrt{1+\frac{2W'_0}{\tilde{W}_{\infty}}}-1\right)}{W'_0}, \tag{35}$$

where, in both equations, we have used $W'_0 = 2E_c^{\mathrm{PT2}}$ and $\tilde{W}_{\infty} = W_{\infty} - E_x$.

II. COMPARISON BETWEEN E_c^{HF} AND E_c^{KS}

Both the HF and the KS states that correspond to the interacting problem introduced in Eq. (4) can be constructed analytically.[14] This quite rare (if not unique) circumstance allows us to establish a detailed comparison between the two theories (see Figs. 3, 5, 6, and 7). Moreover, we discuss both these methods from a site-occupation function theory standpoint [see Figs. 1, 2, and 8 and Eq. (45)]. This is quite usual for the KS theory but rather uncommon for the HF. Before showing the results for the HF and KS correlation energies and their individual contributions (Sec. II B), we review such methods as applied to the Hubbard dimer.

A. Mean-field solutions: An overview

In the non-interacting case, when $U \equiv 0$ in Eq. (4), the solution to the Schrödinger equation is particularly simple. The GS occupation, which can be constructed from the non-interacting solution, is analytically invertible in terms of the potential and reads

$$\Delta v = -\frac{\Delta n}{\sqrt{4-\Delta n^2}}. \tag{36}$$

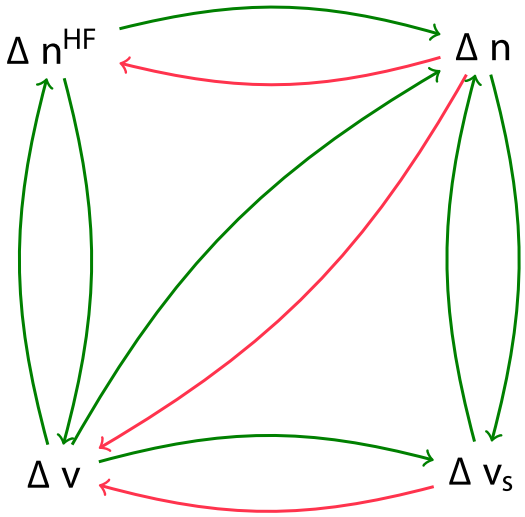

FIG. 1. Schematic of the occupation and external potential functions considered in this work. The green arrows mean that the function in question is known analytically. For example, the function $\Delta n\left(\Delta n^{\mathrm{HF}}\right)$—represented by the uppermost arrow—is known analytically and is plotted in the bottom panel of Fig. 2. By contrast, its inverse, $\Delta n^{\mathrm{HF}}(\Delta n)$, could not be expressed in closed form.

In the Hubbard model community, this case is referred to as the "tight-binding" problem. As this case is relevant for the application of the KS method, and to distinguish the external potential (difference) pertaining to the target interacting problem from its non-interacting effective mapping, we relabel the external potential found from Eq. (36) as "Δv_s" (see also the right edge of Fig. 1).

Consider now the HF Hamiltonian for the Hubbard dimer:

$$\hat{\mathscr{H}}^{\mathrm{HF}} = \hat{\mathscr{T}} + \sum_{i=0,1}\sum_{\sigma} U n_{i\bar{\sigma}}^{\mathrm{HF}} \hat{n}_{i\sigma} + \sum_{i=0,1} v_i \hat{n}_i. \tag{37}$$

In contrast to Eq. (4), in Eq. (37), there is no interaction term and the repulsion is taken into account in a mean field fashion by the central term, $U n_{i\bar{\sigma}}^{\mathrm{HF}}$. On each site, the occupation with spin σ feels the repulsion generated by the spin-$\bar{\sigma}$ occupation of the same site. We reiterate that, contrary to the usual continuum setting, here there is no repulsion between particles of the same spin. In Eq. (37), this central term is reported as converged to the stationary point at which the mean field is generated by the HF occupation.

Furthermore, if we require that the spin up and spin down occupations are equal, we can substitute $n_{i\bar{\sigma}}^{\mathrm{HF}} = n_{i\sigma}^{\mathrm{HF}} = \frac{n_i^{\mathrm{HF}}}{2}$ in Eq. (37), obtaining the corresponding restricted Hartree–Fock (RHF) Hamiltonian,

$$\hat{\mathscr{H}}^{\mathrm{RHF}} = \hat{\mathscr{T}} + \hat{\tilde{\mathscr{V}}}, \tag{38}$$

with

$$\hat{\tilde{\mathscr{V}}} = \sum_{i=0,1} \tilde{v}_i \hat{n}_i, \tag{39}$$

$$\tilde{v}_i = v_i + \frac{U}{2} n_i^{\mathrm{HF}}. \tag{40}$$

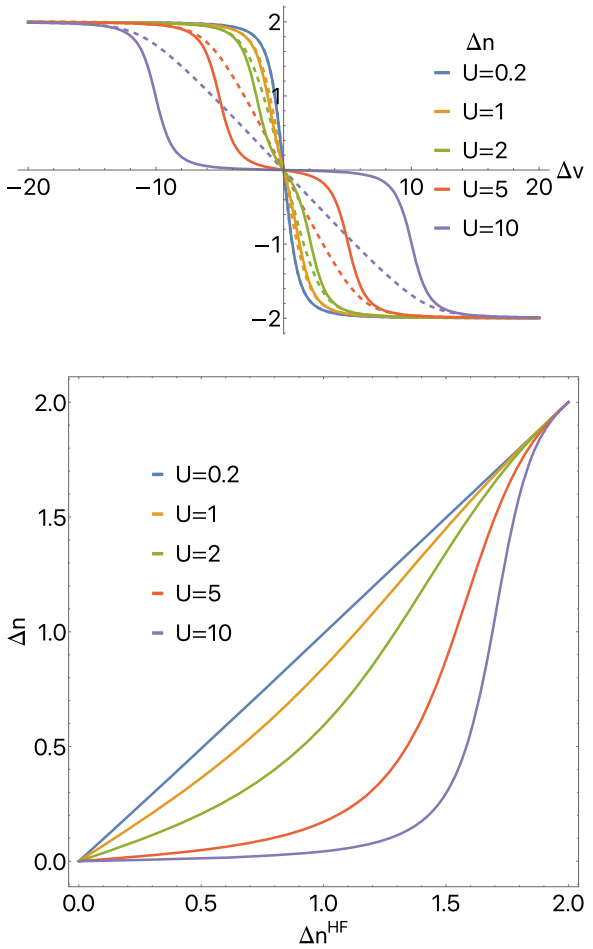

FIG. 2. Upper panel: site occupation differences for the interacting (solid) and the HF (dashed) systems as a function of the external potential difference, Δv, for $U = 0.2, 1, 2, 5$, and 10. Lower panel: interacting site occupation difference, Δn, as a function of the HF one, Δn^{HF}, for $U = 0.2, 1, 2, 5$, and10.

In the following, we will always consider the RHF occupation resulting from Eqs. (38)–(40), referring to it as simply "HF."

Note that, while the eigenvectors of Eq. (4) do not depend on the individual values, v_i, of the external potential but only on their difference, Δv, the energy does depend on the individual v_i. One can also express the energy as a function of Δv and a constant c that represents the gauge choice, $c = v_0 + v_1$, and is typically set to zero. However, setting $v_0 + v_1 = 0$ forces $\tilde{v}_i$ of Eq. (40) to give $\tilde{v}_0 + \tilde{v}_1 = U$ (since the $n_0^{\mathrm{HF}} + n_1^{\mathrm{HF}} = 2$). From Eq. (38), consequently, we can reconstruct the external potential as a function of the HF occupation by altering Eq. (36) to include a mean field repulsion term,

$$\Delta v = -\frac{U}{2}\Delta n^{\mathrm{HF}} - \frac{\Delta n^{\mathrm{HF}}}{\sqrt{4 - \left(\Delta n^{\mathrm{HF}}\right)^2}}. \tag{41}$$

The above function is also invertible and Δn^{HF} can be expressed as a function of $\{U, \Delta v\}$. We avoid reporting it here, but it can

be found together with the other formulas and plots given in this work in a supporting notebook available for download at https://notebookarchive.org/2022-06-1ft9zde.

We now address the adaptation of the mean-field term [Eq. (14)] and of the exchange [Eq. (15)] in the Hubbard dimer setting as follows: first, we define the mean-field repulsion energy in this context as follows:

$$U_H(\Delta n) := \frac{U}{2}\left(1 + \left(\frac{\Delta n}{2}\right)^2\right). \tag{42}$$

Equation (42) for the mean-field energy differs from how usually this term is defined within the Hubbard dimer (see, e.g., Ref. 14). However, given that in the operator $\hat{\mathscr{U}}$, as defined in Eq. (6), there is no interaction between particles of the same spin, it seems to us that defining the mean field term as proportional to the sum of the squares of *half* the site occupation on each site (recalling that we are dealing with a spin-compensated system) is more appropriate. Correspondingly, the exchange contribution in the Hubbard dimer setting for a two-electron spin singlet vanishes.

To conclude this section, in Fig. 1, we visually summarize all the analytical pathways that connect the target interacting state to the two different "non-interacting" reference states. For each reference state, we can construct the external potential from its corresponding GS occupation and vice versa (as sketched in the left and right sides of the picture), whereas the connection between the two reference states works only in the direction from left to right and not the other way around. Indeed, if we could either construct the external potential of the interacting system from the knowledge of the KS one (bottom arrow of the picture) or construct the KS occupation from the knowledge of the HF one (upper arrow of the picture), we would find the external potential of the interacting system as a function of its GS occupation. As already mentioned, this problem has no analytical solution even in this extremely gaunt model system, except in the symmetric case, i.e., $\Delta v = 0$, or in the limit where the interaction energy dominates over the kinetic/hopping one, i.e., $U \to \infty$.

In Fig. 2, we plot the functions Δn and Δn^{HF} along the external potential difference in the upper panel and against each other in the bottom panel. When U is small, e.g., $U = 0.2$, the two occupations differ very slightly, while their difference increases for larger U, as expected. The function Δn vs Δv, shown in the upper panel, can be quite flat for extremely large portions of its domain; on the other hand, the function Δn vs Δn^{HF}, on the bottom panel, appears to be much gentler, at least for intermediate values of U (becoming non-analytical for $U \to \infty$). Thus, from a numerical point of view, it is, in general, much more convenient to invert this latter relation and then use the function Δv vs Δn^{HF} rather than directly inverting the function Δv vs Δn (diagonal of Fig. 1). We see that the two site occupations become equal in the symmetric limit, $\Delta v = 0$, and asymptotically (i.e., for $\Delta v \to \pm\infty$), where in both cases, the interplay between U and Δv vanishes.

B. Individual contributions to the correlation energies

In a spirit similar to that of Ref. 5, in this section, we compare the individual contributions to the HF and the KS correlation energies with one another. We begin by comparing kinetic correlation energies when we fix the external potential. By definition [Eq. (16)], T_s is the minimal kinetic energy for a given density. However, as mentioned previously, when we solve a quantum problem for a given external potential, $n^{\mathrm{HF}} \neq n$. It then becomes interesting to compare the correlation kinetic energy contribution in the two theories, T_c^{HF} and T_c^{KS} [Eq. (11)] as a function of the external potential difference, Δv. This is done in Fig. 3 for different U values. The dashed curve corresponds to SD = HF, while the solid one corresponds to KS (as is the case in all the following figures in this section). Note that $T^{\mathrm{SD}}[\Delta n] = -\sqrt{1 - \left(\frac{\Delta n}{2}\right)^2}$ for any non-interacting reference state, so that actually $T^{\mathrm{KS}} \equiv T^{\mathrm{HF}}$ as a function of a given site occupation. However, if we consider the HF or the KS kinetic energy for a particular external potential, we see that the inequality $T^{\mathrm{KS}} \leq T^{\mathrm{HF}}$ still holds, becoming an equality when the interacting and the HF site occupations become equal ($\Delta v = 0$ and $\Delta v \to \infty$). Furthermore, we observe that for each U there is a turning point in $|\Delta v|$ at which $T_c^{\mathrm{HF}} \equiv 0$ and past which the HF hopping energy is higher than the interacting one, showing first evidence, to our knowledge, of $T_c^{\mathrm{HF}} < 0$. To better understand this result, let us go back to the hopping operator $\hat{\mathscr{T}}$ in Eq. (5). By definition, $\hat{\mathscr{T}}$ favors delocalization of each spin particle over the two sites. In other words, while $\hat{\mathscr{V}}$ tries to localize both particles on the site of lower potential energy and $\hat{\mathscr{U}}$ tries to localize particles of different spin each on one site, $\hat{\mathscr{T}}$ favors the mixture of these states. In this sense, it is going against the action of both $\hat{\mathscr{U}}$ and $\hat{\mathscr{V}}$. Therefore, the expectation value of $\hat{\mathscr{T}}$ is not monotonic in $|\Delta v|$ and reaches its minimum when the two other competitors balance out, roughly at $|\Delta v| \approx U$. On the other hand, in the case of the HF Hamiltonian, the only competing operator is $\hat{\mathscr{V}}$. The effective external potential, $\Delta\tilde{v} = \Delta v + \frac{U}{2}\Delta n^{\mathrm{HF}}$, goes monotonically with Δv. In particular, we find that when $|\Delta v| > U$, $\Delta\tilde{v} \sim \Delta v + (\operatorname{sign}\Delta v)U$, while when $|\Delta v| < U$, $\Delta\tilde{v} \sim \frac{\Delta v}{U}$ (for large enough U). In Fig. 4, $\Delta\tilde{v}$ is plotted for $U = 5$, demonstrating these shifts in different regimes. Consequently, the HF kinetic energy is monotonic in $|\Delta v|$ and its minimum is reached for $\Delta v = 0$. Furthermore, the two kinetic energies have comparable magnitude in the Hubbard dimer, which, combined with their contrasting behavior, results in their crossing around $|\Delta v| \approx U$.

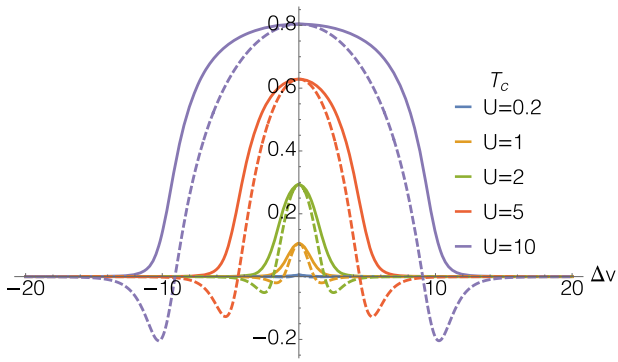

FIG. 3. Correlation kinetic energy contribution T_c^{SD} [Eq. (11)] for the Hubbard dimer as a function of Δv and for $U = 0.2, 1, 2, 5$, and 10. The dashed curve corresponds to SD = HF, while the solid one corresponds to KS.

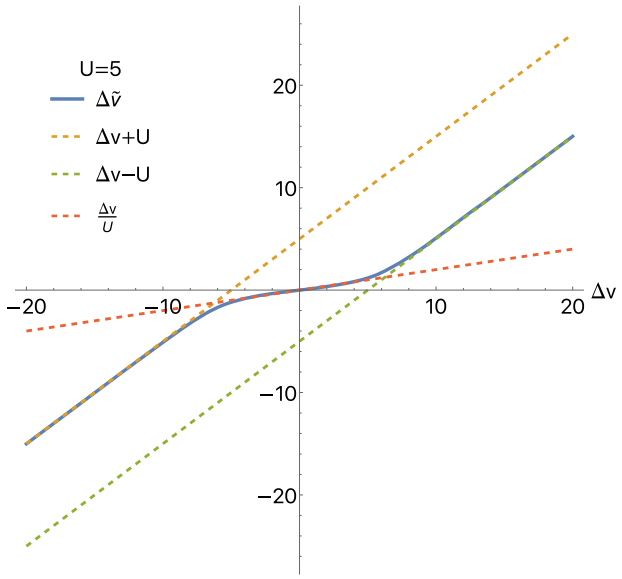

FIG. 4. Effective external potential of the HF Hamiltonian, $\Delta\tilde{v}$ (blue curve), contrasted with $[\Delta v + (\text{sign}\,\Delta v)\,U]$ (orange and green curves) and $\frac{\Delta v}{U}$ (red), for $U = 5$.

Moving on to comparison of U_c^{HF} and U_c^{KS} [Eq. (12)] in Fig. 5, we see that the discrepancy of this energy contribution is systematically larger (in magnitude) in the HF reference state than in the KS one. Note that also U_c^{HF} contains the correction coming from the Hartree term, $U_{H,c}^{\text{HF}} := \frac{U}{2}\left(\left(\frac{\Delta n}{2}\right)^2 - \left(\frac{\Delta n^{\text{HF}}}{2}\right)^2\right)$. Quite interestingly, we find that the indirect Coulomb correlation energy defined as $U_{ind,c}^{\text{SD}} := U_c^{\text{SD}} - U_{H,c}^{\text{SD}}$ is exactly the same in the two reference states, meaning that $U_{ind,c}^{\text{HF}} \equiv U_c^{\text{KS}}$. Therefore, the discrepancy observable in Fig. 5 between the two methods is entirely due to the term $U_{H,c}^{\text{HF}}$, the mean field correction for the HF site occupation being different than the interacting one. Because the comparison is made with fixed external potential, and the HF and KS site occupations typically

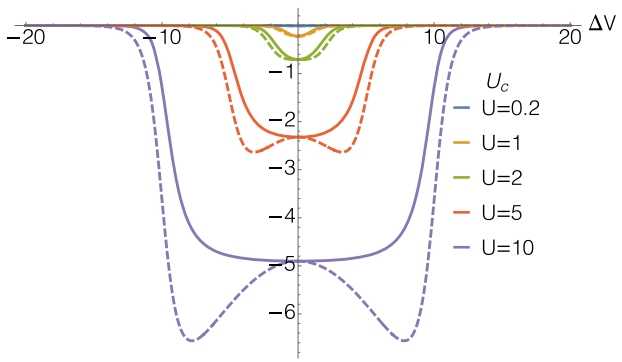

FIG. 5. Correlation Coulomb energy contribution U_c^{SD} [Eq. (12)] for the Hubbard dimer as a function of Δv and for $U = 0.2, 1, 2, 5$, and 10. The dashed curve corresponds to SD = HF, while the solid one corresponds to KS.

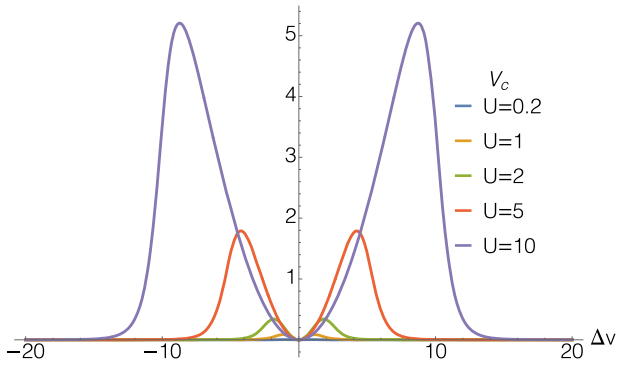

FIG. 6. Correlation potential energy contribution V_c^{HF} [Eq. (13)] for the Hubbard dimer as a function of Δv and for $U = 0.2, 1, 2, 5$, and 10. This contribution is exactly zero for the KS reference.

differ (see Fig. 2), this means, in turn, that the dependence of $U_{ind,c}^{\text{SD}}$ on the site occupation in the two treatments is different.

Finally, we examine how E_c^{HF} and E_c^{KS} compare to one another. Both correlation energies account for the difference between the expectation value of the Hamiltonian operator in the GS and that in the single SD reference state, i.e.,

$$E_c^{\text{SD}} = E - \langle \Phi^{\text{SD}} | \hat{H} | \Phi^{\text{SD}} \rangle, \tag{43}$$

with SD = HF, KS. By virtue of definition (8) and of the variational principle, it is immediate to see that $E_c^{\text{KS}} \leq E_c^{\text{HF}}$. However, as demonstrated above, both U_c^{HF} and T_c^{HF} are less than or equal to their KS counterparts, meaning that $T_c^{\text{HF}} + U_c^{\text{HF}} \leq T_c^{\text{KS}} + U_c^{\text{KS}}$. We conclude that it is the term V_c^{HF} of Eq. (13), shown in Fig. 6, that cancels out a significant portion of the error residing in the other contributions (T_c^{HF} and U_c^{HF}). Thus, adding up all the terms, we indeed retrieve the inequality $E_c^{\text{KS}} \leq E_c^{\text{HF}}$, holding for a given external potential, as seen in Fig. 7. In passing, we note that the maximum of both $|U_c^{\text{HF}}|$ and V_c^{HF} is found near $|\Delta v| \approx U$. This can be explained by the fact that both terms are related to how much the HF site occupation differs from the interacting one (in the case of U_c^{HF}, this is related to the term $U_{H,c}^{\text{HF}}$, as discussed). In fact, as can be deduced from the top

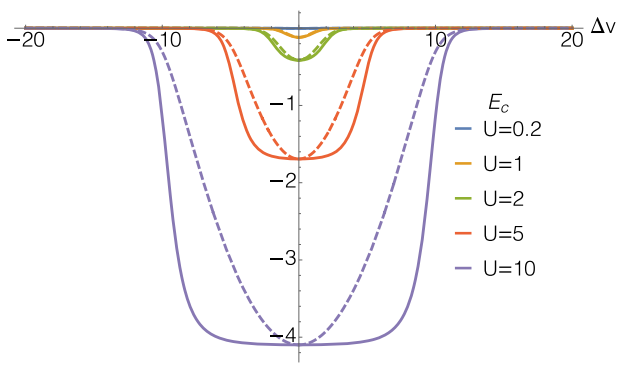

FIG. 7. Total correlation energies E_c^{HF} (dashed) and E_c^{KS} (solid), respectively, Eqs. (10) and (17), for the Hubbard dimer as a function of Δv, for $U = 0.2, 1, 2, 5$, and 10.

panel of Fig. 2, the biggest error in the HF site occupation occurs for values of $|\Delta v|$ lower than, but nearing, U.

Questions remain about how the results illustrated so far for the Hubbard dimer transfer to Coulomb quantum systems in the spatial continuum. Due to the profound difference in nature between the hopping operator and the quantum kinetic energy operator, it is hard to say whether there exist more realistic quantum systems with negative T_c^{HF}. In the case of the usual quantum kinetic energy operator, a negative T_c^{HF} means that the kinetic energy of particles interacting via an effective mean field is higher than the one of electrons interacting coulombically. However, typically, we expect interacting particles to be more sensitive than non-interacting ones to any change in their coordinates, thus being described by a wavefunction whose variation in space is more pronounced and, consequently, has higher kinetic energy. However, in principle, we do not exclude that it might be possible to find rather pathological examples where such an expectation would be contradicted, although none has been found so far in studies focused strictly on cases in which the RHF solution is the lowest-energy HF state.[40] In Ref. 5, the authors study the individual contributions to the correlation energies within the RHF and the KS theories for the molecules Li_2, N_2, and F_2 at equilibrium or larger bond distances. There, the case where $T_c^{\mathrm{HF}} < T_c^{\mathrm{KS}}$ (as in Fig. 3) is never encountered. In other words, in their cases, the HF kinetic energy is typically lower than the KS one for a given external potential and, consequently, lower than the interacting one. However, they also observe that the HF kinetic energy is typically much more sensitive to the geometry than the KS one.

Concerning the remaining contributions, U_c^{SD} and V_c^{HF}, our results are of somewhat general validity: the HF state tends to "overstabilize" the energy by relaxing the density, but the individual contributions to the energy are less in line with the exact ones than their KS counterparts. This is in agreement with what is observed in Ref. 5: $U_{H,c}^{\mathrm{HF}}$ and V_c^{HF} have similar orders of magnitude (with this latter being typically larger, up to a factor of four) and are opposite in sign, while the difference between $U_{c,\mathrm{ind}}^{\mathrm{HF}}$ and U_c^{KS} is between one and three orders of magnitudes smaller (in the Hubbard dimer, as said, this difference is exactly zero). The only *caveat* is that, in non-lattice systems, the HF density is typically more diffuse. This means that $V_c^{\mathrm{HF}} < 0$, as the HF density is less peaked around the nuclei where the nuclear field is more attractive, and that $U_{H,c}^{\mathrm{HF}} > 0$, as the HF mean field repulsion is milder. In our model, a more diffuse density translates in a larger site-occupation difference, i.e., $|\Delta n^{\mathrm{HF}}| \geq |\Delta n|$ (see Fig. 2), resulting in those contributions having the reverse sign, i.e., $V_c^{\mathrm{HF}} > 0$ and $U_{c,H} < 0$.

We now want to consider a scenario that can virtually be realized only within the Hubbard dimer setting. We ask ourselves how the HF and the KS correlation energy functions compare to one another if we match the two site-occupation differences. In this case, as visible in Fig. 8, the opposite inequality appears to hold, i.e.,

$$E_c^{\mathrm{KS}}(U,\Delta n)\big|_{\Delta n\equiv\Delta n^{\mathrm{HF}}} \geq E_c^{\mathrm{HF}}(U,\Delta n^{\mathrm{HF}}). \tag{44}$$

Note that the function $E_c^{\mathrm{KS}}(U,\Delta n)$ is not known analytically and it has been obtained from numerical inversion. On the other hand, the expression for E_c^{HF} can be found analytically and reads

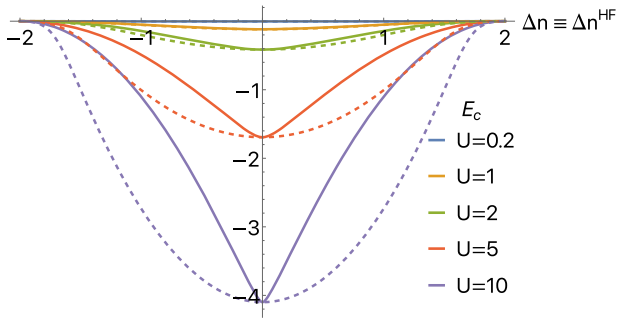

FIG. 8. Total correlation energies E_c^{HF} (dashed) and E_c^{KS} (solid)—Eqs. (10) and (17), respectively—for the Hubbard dimer as a function of the site occupation Δn^{HF} and Δn (set equal), for $U = 0.2, 1, 2, 5$, and 10.

$$E_c^{\mathrm{HF}}(U,x) = \frac{1}{24}\left(-16\,f(U,x)\sin\left(\frac{1}{6}\left(2\cos^{-1}\left(-\frac{U}{2}\frac{g(U,x)}{f(U,x)^3}\right)+\pi\right)\right) + 3Ux^2 + 4U + \frac{48}{\sqrt{4-x^2}}\right), \tag{45}$$

with

$$f(U,x) = \sqrt{3+U^2+3x^2\left(\frac{U}{2}+\frac{1}{\sqrt{4-x^2}}\right)^2},$$
$$g(U,x) = \left(9,+,2U^2-18x^2\left(\frac{U}{2}+\frac{1}{\sqrt{4-x^2}}\right)^2\right),$$

and $x = \Delta n^{\mathrm{HF}}$. Its small-$U$ expansion gives us the Møller–Plesset perturbation[41] series coefficients,

$$E_c^{\mathrm{MP2}}(U,x) = -\frac{1}{256}U^2\left(4-x^2\right)^{5/2}, \tag{46}$$

$$E_c^{\mathrm{MP3}}(U,x) = -\frac{U^3x^2\left(x^2-4\right)^3}{2048}, \tag{47}$$

$$\cdots$$

(where we have reported only the first two, as the coefficients grow in complexity).

Comparison of Eqs. (46) and (47) with the Görling–Levy[28,29] series expansion coefficients, E_c^{GL2} and E_c^{GL3}, reported in Eqs. (88) and (89) of Ref. 14, shows that these coefficients are formally identical in the two perturbation treatments for the Hubbard dimer. The only difference is that, here, they are functions of the HF site occupation, $x = \Delta n^{\mathrm{HF}}$, whereas in the DFT case, they are functions of the interacting site occupation. [Note also that each of the terms in the energy expressions of Eqs. (45)–(47) depends on the square of the site-occupation difference, rather than on the site-occupation difference itself.] Concerning the second-order coefficients, their formal equivalence is due to the formal equivalence of the sum of the

Hartree and exchange terms in the two theories. As for the equivalence between the third-order coefficients, this may simply be due to the lack of same-spin interaction in the model. However, similar investigations in other models are needed to clarify its influence.

To summarize, in this section, we have calculated the *exact* total and partial correlation energies corresponding to the HF or the KS reference states, comparing the resulting pairs. In Sec. III, we shall focus on *approximate* expressions for the correlation energy, which can be used within both theories.

III. PERFORMANCE OF THE LB AND SPL FUNCTIONALS FOR THE HUBBARD DIMER

We previously introduced the practice of adopting density functional approximations developed for the correlation energy in KS-DFT and using them with HF ingredients as a correction to the HF energy. In particular, functionals coming from the so-called adiabatic connection framework, ACMs, have been successfully used in this manner.[33–36] As said, these formulas interpolate between the weak- and strong-interaction expansions of the adiabatic connection integrand, W_λ^{SD}. This function(al) integrates to the desired correlation energy between the two extremes, zero and one, of the interaction strength parameter λ, i.e., $\int_0^1 W_\lambda^{\mathrm{SD}} \mathrm{d}\lambda = E_c^{\mathrm{SD}}$ (with SD = HF, KS). A more detailed treatment of the MP adiabatic connection integrand, W_λ^{HF}, for the Hubbard dimer is currently in preparation. In this context, we focus only on the performances of the adiabatic connection methods corresponding to the LB [Eq. (34)] and the SPL [Eq. (35)] functionals. The validity of such approximations, in the Hubbard dimer setting, can be assessed without introducing any other source of errors, such as the ones coming from using approximate KS orbitals (e.g., PBE,[42] PBE0,[43] etc.) or basis set expansions. These LB and SPL formulas require as ingredients the quantities E_x, E_c^{PT2}, and W_∞. The first one, as said, is exactly zero in our Hubbard dimer, so we have $\tilde{W}_\infty \equiv W_\infty$ in this case. The E_c^{PT2} ingredient corresponds to Eq. (46) for both references (HF and KS), as discussed in Sec. II B.

W_∞ corresponds to the leading term, which is in the order of λ, in the large-λ expansion of $E_c^{\mathrm{SD}}(\lambda U, x)$,

$$\lim_{\lambda\to\infty} E_c^{\mathrm{SD}}(\lambda U, x) \sim \lambda W_\infty^{\mathrm{SD}}. \tag{48}$$

Explicit expressions for W_∞^{SD}'s two different reference states read

$$W_\infty^{\mathrm{HF}}(U, x) = \frac{U}{8}\left(x^2 - 4\right) \tag{49}$$

and

$$W_\infty^{\mathrm{KS}}(U, x) = -\frac{U}{2}\left(1 - \left|\frac{x}{2}\right|\right)^2. \tag{50}$$

Note that the latter expression has been already reported in Eq. (56) of Ref. 14 (as subsequently corrected in the Erratum[44]).

In Fig. 9, we compare how well the LB approximation works for the Hubbard dimer in the context of KS-DFT. In Fig. 10, we report instead the performance of the LB functional used with HF ingredients as a correction to the traditional correlation energy, E_c^{HF}. Finally, in Fig. 12, we plot the difference $\Delta E_c = \left(E_c - E_c^{\mathrm{LB}}\right)$ for each method. As is visible, for a large portion of the parameter space,

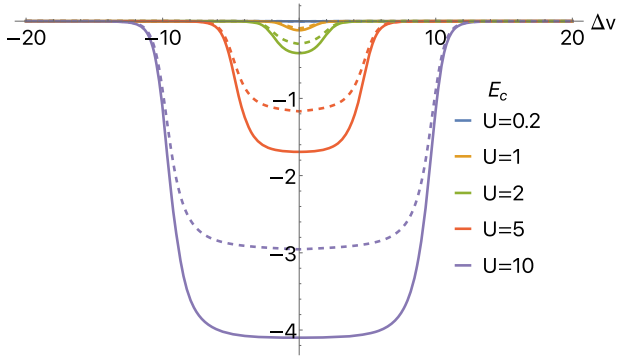

FIG. 9. Exact KS correlation energy E_c^{KS} (thick) and its approximation using the LB functional [Eq. (34)] (dashed) for the Hubbard dimer with ingredients $W_0' = 2\,E_c^{\mathrm{GL2}}$, $W_\infty = W_\infty^{\mathrm{KS}}(U, x)$, and $x = \Delta n(\Delta v)$, for $U = 0.2, 1, 2, 5$, and 10.

the LB approximation for the Hubbard dimer works better for the HF reference state and as a correction to the traditional correlation energy than for the KS ones. In fact, the only region where the LB approximation works better for the KS correlation energy corresponds to weakly correlated systems, where the external potential difference dominates over the repulsion term. We also note that just as for the HF kinetic energy (see Fig. 3), there is a particular combination of U and Δv for which the LB approximation yields the exact HF correlation energy.

As a further point, we propose to investigate the performance of the LB functional adopting mixed ingredients—the W_∞ associated with the KS-DFT correlation energy but with the HF site-occupation difference as input. This may seem quite an arbitrary choice. However, it is precisely the way in which said ACMs have mostly been used, for a very pragmatic reason. W_∞^{KS} has been known for quite a long time,[30] and an excellent approximation to it in the form of a gradient expansion has been developed since.[45] W_∞^{HF} has been introduced only recently[38] and gradient expansion approximations to it have just been devised.[46] The mixed LB functional thus obtained is used as a correction to the HF energy. Its performance for the Hubbard dimer is shown in Fig. 12, contrasted with the internally

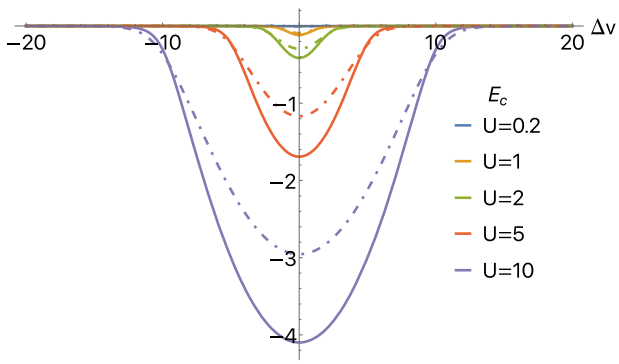

FIG. 10. Exact HF correlation energy E_c^{HF} (thick) and its approximation using the LB functional [Eq. (34)] (dotted-dashed) for the Hubbard dimer with ingredients $W_0' = 2\,E_c^{\mathrm{MP2}}$, $W_\infty = W_\infty^{\mathrm{HF}}(U, x)$, and $x = \Delta n^{\mathrm{HF}}(\Delta v)$, for $U = 0.2, 1, 2, 5$, and 10.

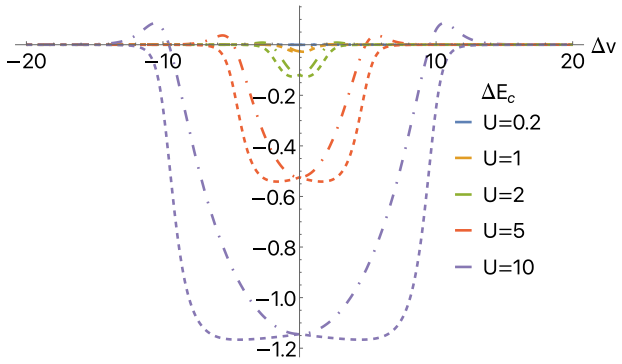

FIG. 11. Difference $\Delta E_c^{\mathrm{LB}} = \left(E_c - E_c^{\mathrm{LB}}\right)$ for HF reference state (dotted-dashed) and for the KS reference state (dashed) at various U, as a function of Δv.

consistent strategy already discussed, as a function of the HF site occupation. For most of the site-occupation domain, this mixed-ingredient combination is quite inaccurate and greatly worsening in performance. There is only a small region where the mixed-ingredient combination yields better estimates of the HF correlation energy. This region corresponds to the outer edges of the domain of Δn^{HF}, i.e., the weakly correlated cases where $|\Delta n^{\mathrm{HF}}|$ approaches two.

Therefore, in the Hubbard dimer setting, it is clear that the LB functional (as well as the SPL functional, see discussion below) works better when the appropriate strong-interaction ingredient for the HF reference, i.e., W_∞^{HF} is adopted, rather than W_∞^{KS}, for high- and intermediate-correlation regimes. This is somewhat reassuring, as it shows that these adiabatic connection methods work as intended, giving better results when consistent ingredients are used and not benefiting from an error cancellation between the KS ingredient W_∞^{KS} and the HF site-occupation input.

The trends observed for the SPL functional across the Hubbard dimer parameter space were qualitatively equivalent to those observed for the LB functional, although the SPL estimate of the correlation energy appears to be larger than the LB one everywhere for both the KS and the HF references cases. Note that, in the KS case, both LB and SPL functionals appear to bound the exact correlation energies from above. This, in turn, means that the SPL correlation energy error is everywhere larger than the LB one, i.e., $|\Delta E_c^{\mathrm{KS,SPL}}| > |\Delta E_c^{\mathrm{KS,LB}}|$ with $\Delta E_c^{\mathrm{KS,ACM}} = E_c^{\mathrm{KS}} - E_c^{\mathrm{KS,ACM}}$ and ACM = LB, SPL. As an example, the maximum error for $U = 10$ is 1.14 E_h for the LB functional and 1.42 E_h for the SPL one.

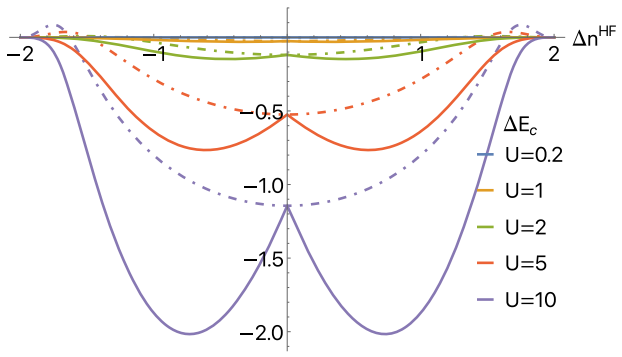

FIG. 12. Difference $\Delta E_c^{\mathrm{LB}} = \left(E_c - E_c^{\mathrm{LB}}\right)$ for HF reference state (dotted-dashed) and for E_c^{LB} with mixed ingredients, namely, $W_0' = 2\,E_c^{\mathrm{MP2}}$, $W_\infty = W_\infty^{\mathrm{KS}}(U, x)$, and $x = \Delta n^{\mathrm{HF}}$, as a correction to the HF energy (thick), at various U, as a function of Δn^{HF}.

As for the case of the HF reference, both functionals have a turning point around the value $|\Delta v| \approx U$. In the strong-correlation regime, when $|\Delta v| < U$, they underestimate (in magnitude) the exact correlation energy. Past the turning point, when $|\Delta v| > U$, they "overshoot" it. This, in turn, means that the SPL correlation energy error is larger than the LB one, $|\Delta E_c^{\mathrm{HF,SPL}}| > |\Delta E_c^{\mathrm{HF,LB}}|$ in the more strongly correlated cases where $|\Delta v| < U$. In the weakly correlated range of the parameter space (i.e., where $|\Delta v| > U$), we have instead $|\Delta E_c^{\mathrm{HF,SPL}}| < |\Delta E_c^{\mathrm{HF,LB}}|$. Finally, the use of mixed ingredients worsens the performance of the SPL functional in a manner essentially analogous to that observed for the LB case in Fig. 12. The fact that the two different functionals show such a close similarity of trends across the Hubbard dimer parameter space may indicate that the common rationale underpinning both functionals largely determines their performances, despite their differences. A detailed account of the results of the SPL functional, similar to those shown in Figs. 9–12 for the LB one, can be found in the supporting notebook available at https://notebookarchive.org/2022-06-1ft9zde.

IV. CONCLUSIONS

We have provided an analytical comparison between HF and KS-DFT methods for the Hubbard dimer model. One of the most striking findings within this model is that the indirect interaction energies for the two methods, $U_{c,\mathrm{ind}}^{\mathrm{SD}}$, are exactly the same at a given external potential. In line with Ref. 5, our results show that the HF solution can "overstabilize" the energy through the external potential by relaxing the density (site occupation). However, the separate contributions to the energy typically deviate more from the corresponding interacting ones than their KS counterparts (see Figs. 5 and 6). A notable exception is our demonstration of the change in sign in the HF kinetic correlation, which we understand to be a novel finding and contrary to intuitive predictions of its behavior. Furthermore, as the mapping between external potential and HF site occupation is analytically invertible, unlike the interacting case, it is possible to obtain the exact correlation energy that corrects the HF approximation as a function of the HF density in a pure site-occupation function theory (SOFT) spirit [see Eq. (45)].

A natural extension of this work for future consideration is calculating the correlation energy for the Hubbard dimer in an unrestricted Hartree–Fock (UHF) framework. As shown in Ref. 14, in the strong-correlation regime ($|\Delta v| < U$), the UHF site occupation is much closer to the interacting one than the RHF site occupation and the Coulson–Fisher point—where restricted and unrestricted HF energies coincide—takes place at $|\Delta V| \approx U$. Therefore, the profile of the correlation contributions T_c^{HF}, U_c^{HF}, and V_c^{HF} with the UHF reference is expected to differ significantly in the strong-correlation range of the domain of Δv and around the Coulson–Fisher point. In fact, in a similar model system used to study transmission through an Anderson junction, a dramatic difference in the prediction of the exact susceptibility was found according to whether a restricted or an unrestricted solution was used, favoring the symmetry-broken

approach.[47] For more consistent contextualization within other work,[5,40,47] and to examine carefully how symmetry breaking affects the sign of T_c^{HF}, direct comparison of RHF and UHF will be required.

On the subject of adiabatic connection methods, we have assessed the performances of the LB and SPL functionals, finding that, for the more strongly interacting cases, they work better as approximations to E_c^{HF}, rather than as approximations to E_c^{KS}, as originally intended. Note that, in our assessment, we were able to adopt the exact strong-interaction ingredient corresponding to the HF reference (W_∞^{HF}). This is not ordinary. In fact, several works pioneering the application of ACMs as a correction to the HF energy used (a model for) the DFT strong-interaction ingredient, W_∞^{KS}, with the HF density.[33–35] The only exception is a recent study in which an empirical model for W_∞^{HF} is adopted.[36] In turn, as shown in Fig. 12, the use of W_∞^{KS} with the HF density greatly worsens the performances of the ACMs considered, supporting the view that an improvement of their performances on real molecules might follow from using the approximation for the HF strong-interaction ingredient that has recently become available.[46]

In our comparison of HF and KS theories within the Hubbard dimer, we have focused exclusively on the correlation part of the energy. Nonetheless, our conclusions on how these methods compare from a formal point of view should not vary much by the inclusion of the exchange energy. In fact, generally, the exact exchange energy in the two references is expected to differ only slightly.[5] As for how the examined ACMs perform according to which reference is used (HF or KS), the inclusion of the exchange energy term does not affect our conclusions because these methods recover full exact exchange (in other words, the exchange energy term is merely a constant shift). However, the situation in which one calculates the self-consistent density coming from the chosen ACM applied within the KS-DFT framework would be different. This would give an approximation for the KS quantities input in the correlation energy functional that would reflect on its outcome, as well as on the exchange energy. Since the HF framework for the ACMs demands that the correlation energy is added as a post-self-consistent-field (post-SCF) correction using HF orbitals as input, to compare the performances of these interpolations across the two methods, we have considered only their application on exact KS quantities and not their self-consistent-field solution. Nonetheless, this is an aspect to keep in mind since the way in which these ACMs can be used in actual KS-DFT calculations requires either an underlying density functional model to determine approximate KS orbitals or an SCF implementation. An investigation in the Hubbard dimer setting, especially in light of the computational cost for an SCF implementation on real molecules, could be instructive. In fact, an SCF implementation of these ACMs has been carried out only very recently and tested for a few simple chemical species (Ne, CO, and H_2).[48] Follow-up work, in which we present a detailed analysis of the adiabatic connection integrand corresponding to the HF reference [Eq. (29)][38] for the Hubbard dimer, is currently in progress.

ACKNOWLEDGMENTS

We are grateful for fruitful discussions with Dr. Juri Grossi. This work was supported by the U.S. Department of Energy, National Nuclear Security Administration, Minority Serving Institution Partnership Program, under Award No. DE-NA0003866. We acknowledge all indigenous people local to the site of the University of California, Merced, including the Yokuts and Miwuk. We embrace their continued connection to this region and thank them for allowing us to live, work, learn, and collaborate on their traditional homeland (see https://www.hypugaea.com/acknowledgments).

AUTHOR DECLARATIONS

Conflict of Interest

The authors have no conflicts to disclose.

Author Contributions

Sara Giarrusso: Conceptualization (equal); Data curation (lead); Formal analysis (lead); Methodology (lead); Validation (lead); Visualization (lead); Writing – original draft (lead); Writing – review & editing (equal). **Aurora Pribram-Jones:** Conceptualization (equal); Formal analysis (supporting); Funding acquisition (lead); Methodology (supporting); Project administration (lead); Resources (lead); Supervision (lead); Validation (supporting); Writing – review & editing (equal).

DATA AVAILABILITY

The data that support the findings of this study are available from the corresponding author upon reasonable request.

REFERENCES

[1] K. Sharkas, J. Toulouse, and A. Savin, J. Chem. Phys. **134**, 064113 (2011).
[2] S. Ghosh, P. Verma, C. J. Cramer, L. Gagliardi, and D. G. Truhlar, Chem. Rev. **118**, 7249 (2018).
[3] E. Giner, B. Pradines, A. Ferté, R. Assaraf, A. Savin, and J. Toulouse, J. Chem. Phys. **149**, 194301 (2018).
[4] S. Vuckovic, S. Song, J. Kozlowski, E. Sim, and K. Burke, J. Chem. Theory Comput. **15**, 6636 (2019).
[5] O. V. Gritsenko, P. R. T. Schipper, and E. J. Baerends, J. Chem. Phys. **107**, 5007 (1997).
[6] Z.-F. Liu and K. Burke, Phys. Rev. A **79**, 064503 (2009).
[7] M. Seidl, J. P. Perdew, and M. Levy, Phys. Rev. A **59**, 51 (1999).
[8] J. Hubbard, Proc. R. Soc. London, Ser. A **276**, 238 (1963).
[9] E. H. Lieb and F. Y. Wu, Phys. Rev. Lett. **20**, 1445 (1968).
[10] A. Montorsi, *The Hubbard Model: A Reprint Volume* (World Scientific, 1992).
[11] I. Theophilou, F. Buchholz, F. G. Eich, M. Ruggenthaler, and A. Rubio, J. Chem. Theory Comput. **14**, 4072 (2018).
[12] L. Lacombe and N. T. Maitra, Phys. Rev. Lett. **124**, 206401 (2020).
[13] A. Marie, H. G. Burton, and P.-F. Loos, J. Phys.: Condens. Matter **33**, 283001 (2021).
[14] D. J. Carrascal, J. Ferrer, J. C. Smith, and K. Burke, J. Phys.: Condens. Matter **27**, 393001 (2015).
[15] A. J. Cohen and P. Mori-Sánchez, Phys. Rev. A **93**, 042511 (2016).
[16] Z.-J. Ying, V. Brosco, G. M. Lopez, D. Varsano, P. Gori-Giorgi, and J. Lorenzana, Phys. Rev. B **94**, 075154 (2016).
[17] D. J. Carrascal, J. Ferrer, N. Maitra, and K. Burke, Eur. Phys. J. B **91**, 142 (2018).
[18] B. Senjean, M. Tsuchiizu, V. Robert, and E. Fromager, Mol. Phys. **115**, 48 (2017).
[19] K. Deur, L. Mazouin, and E. Fromager, Phys. Rev. B **95**, 035120 (2017).
[20] J. C. Smith, A. Pribram-Jones, and K. Burke, Phys. Rev. B **93**, 245131 (2016).

[21] P. R. T. Schipper, O. V. Gritsenko, and E. J. Baerends, Theor. Chim. Acc. **99**, 329 (1998).
[22] R. van Leeuwen, Adv. Quantum Chem. **43**, 25 (2003).
[23] K. J. H. Giesbertz and E. J. Baerends, J. Chem. Phys. **132**, 194108 (2010).
[24] J. Harris and R. O. Jones, J. Phys. F: Met. Phys. **4**, 1170 (1974).
[25] O. Gunnarsson and B. I. Lundqvist, Phys. Rev. B **13**, 4274 (1976).
[26] D. C. Langreth and J. P. Perdew, Solid State Commun. **17**, 1425 (1975).
[27] D. C. Langreth, Phys. Rev. Lett. **52**, 2317 (1984).
[28] A. Görling and M. Levy, Phys. Rev. B **47**, 13105 (1993).
[29] A. Görling and M. Levy, Phys. Rev. A **50**, 196 (1994).
[30] M. Seidl, Phys. Rev. A **60**, 4387 (1999).
[31] P. Gori-Giorgi, G. Vignale, and M. Seidl, J. Chem. Theory Comput. **5**, 743 (2009).
[32] M. Seidl, P. Gori-Giorgi, and A. Savin, Phys. Rev. A **75**, 042511 (2007).
[33] E. Fabiano, P. Gori-Giorgi, M. Seidl, and F. Della Sala, J. Chem. Theory Comput. **12**, 4885 (2016).
[34] S. Vuckovic, P. Gori-Giorgi, F. Della Sala, and E. Fabiano, J. Phys. Chem. Lett. **9**, 3137 (2018).
[35] S. Giarrusso, P. Gori-Giorgi, F. Della Sala, and E. Fabiano, J. Chem. Phys. **148**, 134106 (2018).
[36] T. J. Daas, E. Fabiano, F. Della Sala, P. Gori-Giorgi, and S. Vuckovic, J. Phys. Chem. Lett. **12**, 4867 (2021).
[37] K. Pernal, Int. J. Quantum Chem. **118**, e25462 (2018).
[38] M. Seidl, S. Giarrusso, S. Vuckovic, E. Fabiano, and P. Gori-Giorgi, J. Chem. Phys. **149**, 241101 (2018).
[39] T. Helgaker, P. Jorgensen, and J. Olsen, *Molecular Electronic-Structure Theory* (John Wiley & Sons, 2014).
[40] S. Crisostomo, M. Levy, and K. Burke, "Can the Hartree-Fock kinetic energy exceed the exact kinetic energy?" arXiv:2206.11372. (2022).
[41] C. Møller and M. S. Plesset, Phys. Rev. **46**, 618 (1934).
[42] J. P. Perdew, K. Burke, and M. Ernzerhof, Phys. Rev. Lett. **77**, 3865 (1996).
[43] C. Adamo and V. Barone, J. Chem. Phys. **110**, 6158 (1999).
[44] D. Carrascal, J. Ferrer, J. Smith, and K. Burke, J. Phys.: Condens. Matter **29**, 019501 (2016).
[45] M. Seidl, J. P. Perdew, and S. Kurth, Phys. Rev. A **62**, 012502 (2000).
[46] T. J. Daas, D. P. Kooi, A. J. A. F. Grooteman, M. Seidl, and P. Gori-Giorgi, J. Chem. Theory Comput. **18**, 1584 (2022).
[47] Z.-F. Liu, J. P. Bergfield, K. Burke, and C. A. Stafford, Phys. Rev. B **85**, 155117 (2012).
[48] S. Śmiga, F. Della Sala, P. Gori-Giorgi, and E. Fabiano, arXiv:2202.11531 (2022).